H. Salzmann, K. Hirsch, P. Nielsen, C. Gowers, A. Gadd, M. Gadeberg,
H. Murmann and C. Schrodter

First Results from the LIDAR-Thomson Scattering System on JET

First Results from the LIDAR-Thomson Scattering System on JET

H. Salzmann[1], K. Hirsch[1], P. Nielsen, C. Gowers, A. Gadd, M. Gadeberg, H. Murmann[2] and C. Schrodter[3]

JET-Joint Undertaking, Culham Science Centre, OX14 3DB, Abingdon, UK

[1]*Institut für Plasmaforschung, Universitat Stuttgart, 7000 Stuttgart 80, FRG*
[2]*Max-Planck Institut für Plasmaphysik, 8046 Garching, FRG*
[3]*Max-Planck-Institut für Quantenoptik, 8046 Graching, FRG*

FIRST RESULTS FROM THE LIDAR-THOMSON

SCATTERING SYSTEM ON JET

H Salzmann[+], K Hirsch[+], P Nielsen, C Gowers,

A Gadd, M Gadeberg, H Murmann*, C Schrödter[o]

JET Joint Undertaking, Abingdon, Oxon OX14 3EA, UK

[+] On attachment from Institut für Plasmaforschung, Universität Stuttgart,
7000 Stuttgart 80, FRG

* Max-Planck-Institut für Plasmaphysik, 8046 Garching, FRG

[o] Max-Planck-Institut für Quantenoptik, 8046 Graching, FRG

ABSTRACT

The LIDAR Thomson Scattering System on the JET Tokamak is described. First electron temperature profile measurements obtained with this new diagnostic technique are presented.

INTRODUCTION

The application of 180° Thomson scattering using short (~ 300 ps) laser pulses for measuring electron temperature and density profiles in large fusion devices was proposed in [1]. With the short laser pulse method, spatial resolution along the laser beam is in principle achieved by high-speed detection techniques allowing time-of-flight measurements [2]. This LIDAR (Light Detection and Ranging) technique was applied for the first time on the JET tokamak.

THE LIDAR THOMSON SCATTERING SYSTEM

Figure 1 shows the optical set-up of the diagnostic. A ruby laser pulse of 220 ps duration is directed radially into the tokamak vessel in the equatorial plane and dumped on a carbon tile at the inner torus wall. The laser beam inside the vessel has a constant diameter of 50 mm. During the measurements described here, the laser (JK LASERS (Lumonics)

Rugby, UK), capable of 5 J operation at up to 0.5 Hz repetition rate, was
operated at 2 J and single shot.

a) Laser

The laser consists of an actively mode-locked oscillator, two single
pulse selector stages (Pockels cell shutters) in series, four
amplifiers, and a dye flow cell to reduce further the power of the
spurious background pulses leaking through the Pockels cell shutters.

b) Collection Optics

The backscattered light is collected by a folded spherical mirror
system through an array of six windows surrounding the central laser
input window on the JET vessel. Its effective solid angle of
collection is 5.5×10^{-3}sr. The collection optics and the labyrinth
mirror system, which transmits the collected light through the 2.2 m
thick biological shield, is shared with the single spatial point 90°
Thomson scattering system on JET [3], for which it was constructed.
The two collected light beams are separated from each other in the
entrance slit plane of the polychromator of the single point scattering
system. The entrance slit is surrounded by a broadband mirror which
directs approximately 95% of the scattered light from the LIDAR laser
beam into the LIDAR polychromator.

c) Polychromator

The three main features of the LIDAR polychromator are, extremely high
optical throughput of 1 cm²sr, high average transmission of the six
spectral channels (about 70%) and rejection of ruby laser stray light
by a factor greater than 10^5. This performance is achieved with a
filter polychromator in which the incident light is shone onto a stack
of short wave pass interference edge filters with decreasing cut on
wavelengths, the filters being tilted slightly with respect to each
other [4]. The transmission bandwidth of a spectral channel observing
reflected light from this filter stack is defined by the cut-on
wavelengths of two adjacent filters of the stack and by a suitably
chosen coloured glass filter in front of each detector. Additional
interference filters in front of each detector improve further the
rejection of stray ruby laser light. The collection optics, which is
illuminated homogenously by scattered light during the passage of the

-2-

laser pulse through the plasma, is imaged onto the filter stack. In
this way slight variations of the cut-on wavelengths across the surface
of the 200 mm diameter edge filters, are averaged in the same way when
the scattering volume moves through the plasma. In the course of the
first measurements, reported here, only four of the six available
spectral channels were used. Their transmission bands were 660-626 nm,
639-601 nm, 598-534 nm and 530-480 nm, respectively.

d) Detectors and Digitizers

The high speed detection of the backscattered light pulse is
accomplished using proximity focused MCP photomultipliers (ITT F 4128)
with 20 mm diameter photocathode. The output signals are registered by
TEK 7912 AD transient digitisers with 7 A 29 vertical amplifier
plugs-in. The overall bandwidth of the complete detection and
registration system is approximately 700 MHz.

e) Stray Light Suppression

Ruby laser stray light pulses arriving at the detectors before the
scattered signal are suppressed very effectively (by a factor of 10^{13}
/4/) by gating the photocathode to MCP gap of the detectors. The flat
top of the gate is about 30 ns long and the ringing, coupled to the
detector output by the 10 ns risetime/150 V amplitude gating pulse,
could be kept to below 10 mV. An intense stray light pulse occurs
after the measurement when the laser pulse strikes the carbon tile dump
at the Torus inner wall. This stray light burst causes a 300 V/0.5 ns
electrical pulse at the output of the detectors and a high speed, pulse
clipping diode circuit in the signal lead is used to protect the
vertical amplifier plug-ins of the digitizers [5].

RESULTS

Figure 2 shows an overlay of the detector signals recorded by the
digitizers both when the laser was fired during a JET pulse (full curve)
and when no plasma was present in the JET vacuum vessel (dashed curve).
The baselines prior to gating on the detectors appear in region 1.
An unusual stray light source was encountered when the initial dataset was
obtained. It can be seen immediately after the detectors were gated on
(region 2). A monotonically decaying "stray light" signal was observed by
the detectors leading to a distinct 'switch on' peak during the rise of the

-3-

gating pulse. The switch on peak was most pronounced in the signal displayed on digitizer 1, while the slow decay was most clearly seen from digitizers 2 and 3. This 'cw background' signal was shown to be due to spectrally broadband radiation created by spurious ruby laser light incident on a (temporary) black cardboard mask surrounding the laser input mirror (figure 1). The effect of this background radiation on the results was small and in the future it will be avoided completely by imaging the laser output cross section onto this mirror.

Comparison of the stray light signals with the measurement signals in region 3 shows that plasma radiation constitutes only a very small source of background radiation. This is one of the merits of the LIDAR system and is a direct result of using a short integration time in the detection system. Thus, the difference between the continuous and dashed curves in region 4 is predominently due to the scattered light from laser pulse as it propagates through the plasma.

The signal traces are effectively terminated when the main laser pulse hits the inner torus wall and produces a very intense light pulse. The writing speed of the digitizer is inadequate to follow the rapidly rising (-ve) waveform and the trace disappears from the screen at t ~ 48 ns, figure 2. The fact that no discrete ruby laser stray light pulses are detected during the time of measurement (a time window starting ~ 17 ns before the termination of the signal traces), indicates that the suppression of the spurious background laser pulses in front of the main laser pulse, in combination with the rejection ratio of the polychromator, is sufficient to allow unperturbed measurements. The signal to background ratio of the laser emission was measured generally to be better than 10^8. However, 2 ns before the main pulse, a spurious pre-pulse of only a factor of 10^4 less than the main pulse had been measured. The effect of this is visible on digitizer number 1 at 46 ns. This pre-pulse has since been removed by more careful setting up of the laser oscillator.

The scattered light signals from figure 2 have been time correlated using the data obtained from a test experiment in which the peak of the stray termination pulse was displayed by using optical attenuation in front of each detector. The time marker so obtained is also indicated in figure 2. In this first analysis, the electron temperature has been fitted to each 500 ps time averaged segment of the channel data in region 4. The resultant T_e profile is shown in figure 3a where it is compared with the partial T_e profile obtained from the JET ECE diagnostic [6]. At this time

-4-

during the discharge ~ 6 MW of RF heating were being applied to the plasma, producing a moderately high central electron temperature.

In contrast figure 3b shows a low T_e case just after pellet injection in which a central electron temperature of a factor of 4 lower is indicated. Once again good agreement between the profile data from the two diagnostics is obtained. In fact the LIDAR system has been used successfully to date over the 0.2-5 keV temperature range. Also from figure 3b, since the temperature gradient around 2.6 to 2.8 m appears rather steep, it indicates that the spatial resolution of the diagnostic is in the range 0.10-0.15 m as expected. Unfortunately, absolute density profiles were not obtained during these initial experiments because the vignetting effects associated with the particular laser beam profile in use at the time could not be adequately assessed. This will not be the case in the future when the proper input optical system is installed and an in vessel calibration has been conducted.

CONCLUSION

The first electron temperature profiles have been obtained with the novel LIDAR Thomson Scattering diagnostic on the JET Tokamak.

The full T_e profiles are in good agreement over a wide range of plasma conditions with partial profiles obtained by the ECE technique.

A spatial resolution for the diagnostic of 0.10-0.15 m is indicated with this preliminary data set.

ACKNOWLEDGEMENT

REFERENCES

[1] H Salzmann, K Hirsch, Rev Sci Instr 55 (84), 457.

[2] R Kristal, Diagnostics for Fusion Experiments, Varenna 1978, p 617, EUR 6123.

[3] P Nielsen, Course on Diagnostic for Fusion Reactor Conditions, Varenna 1982, Vol 1, p 225, EUR 8351-1EN.

[4] C Gowers, M Gadeberg, K Hirsch, P Nielsen, H Salzmann et al, Course and Workshop on Basic and Advanced Fusion Plasma Diagnostic Techniques, Varenna 1986, page 205, Vol 2.

[5] J Bundgaard et al, private communication.

[6] A E Costley, E A M Baker, M Brusati, D V Bartlett et al, in Controlled Fusion and Plasma Physics (Proc 12th European Conference, Budapest 1985) 9F-I (1985) 227.

JET load assembly   Path of
                         laser pulse

Scattered light
to roof lab.

vacuum vessel

Laser input
mirror

Collection
mirrors

Laser pulse
at some instant

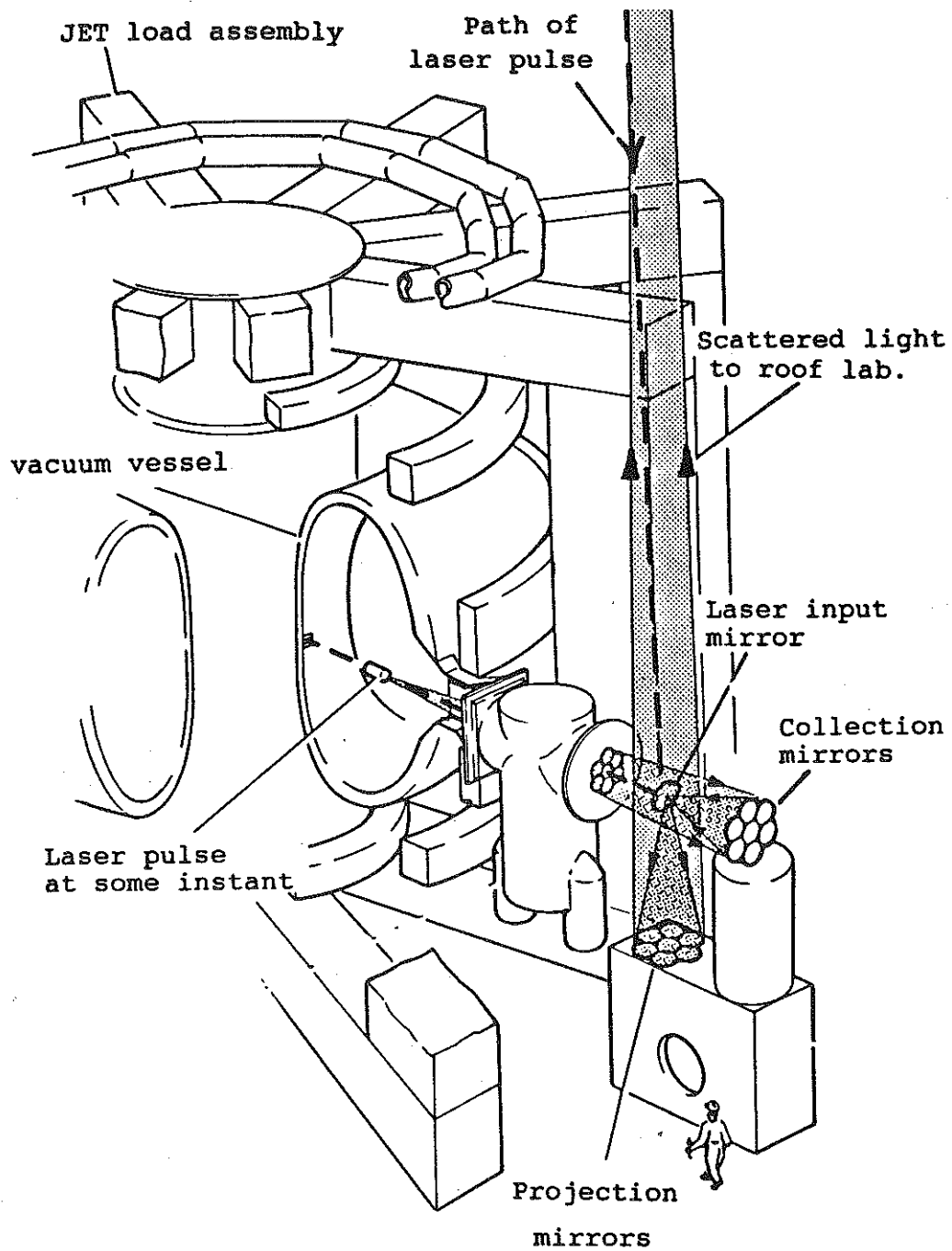Projection

mirrors

Fig. 1 Schematic of input and collection optics on JET.
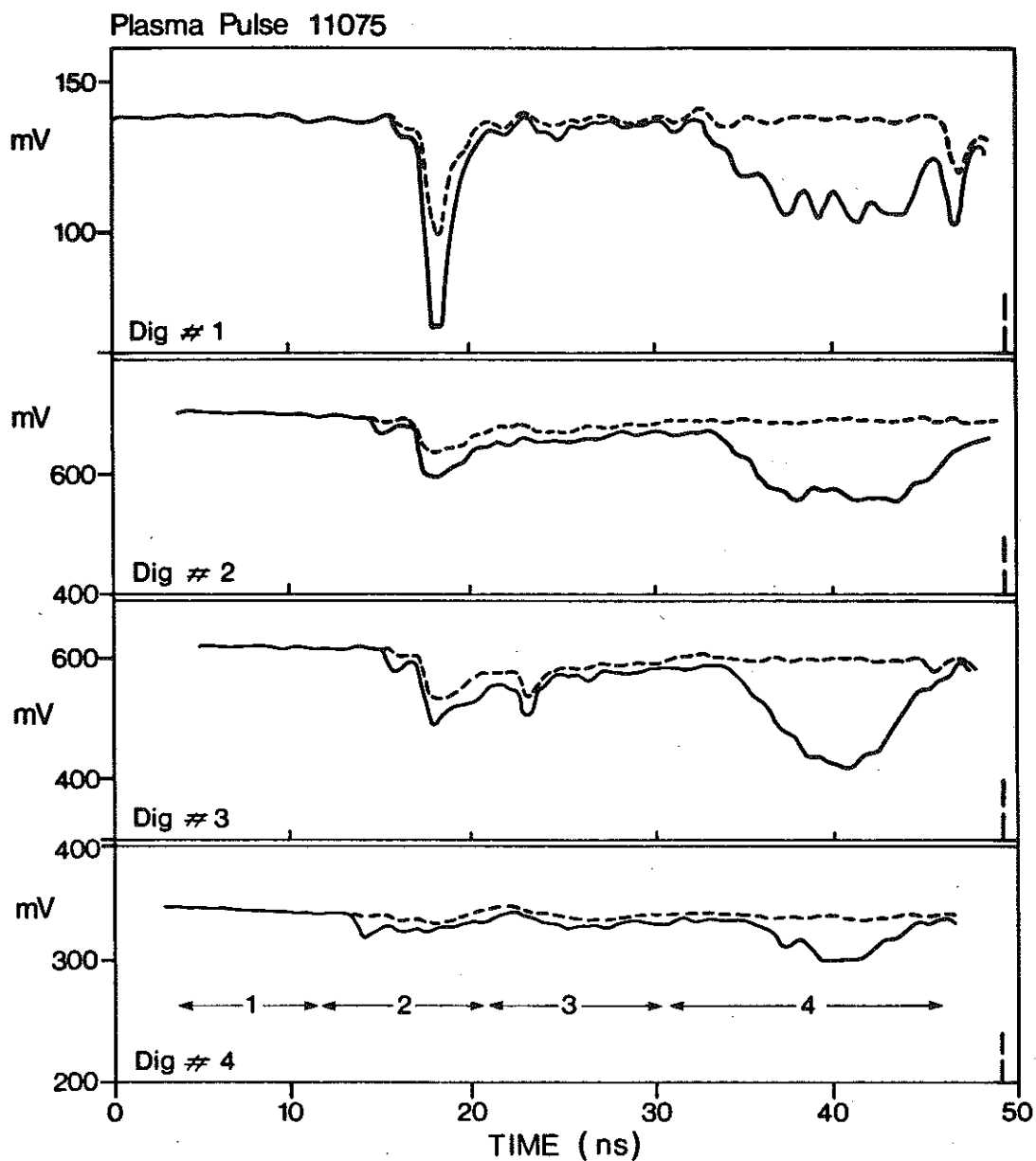
Fig. 2 Signals output by the digitizers a) full curve-during plasma pulse
                                        b) dashed curve-no plasma (laser
                                            only)

Region 1 shows detector output prior to gating

Region 2 shows detector output during gating on

Region 3 shows detector output showing plasma light level

Region 4 shows detector output during period laser pulse traverses
plasma

The vertical bar indicates the fiducial marker for each digitizer
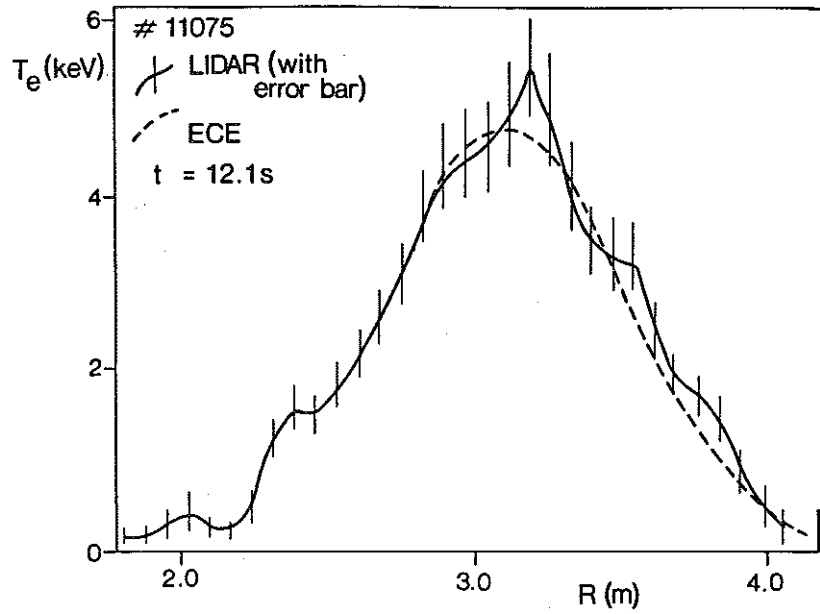signal.
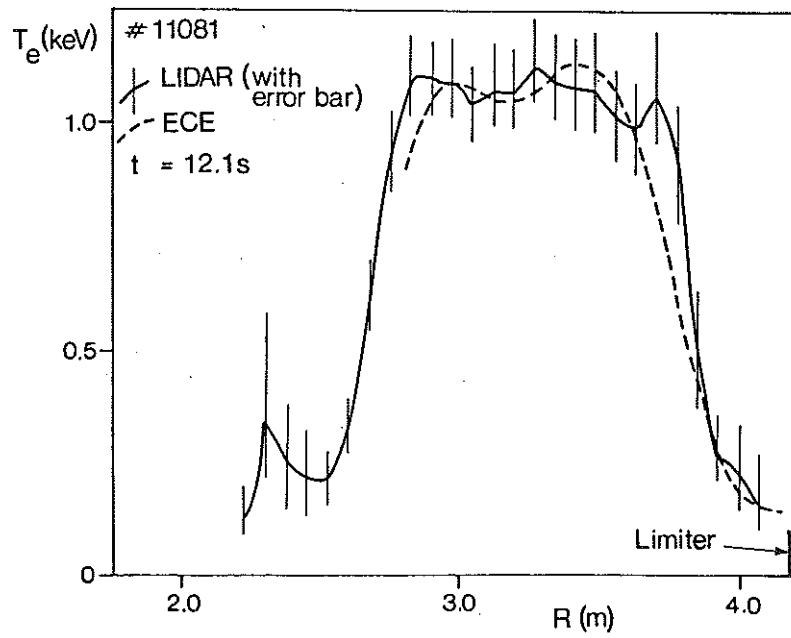
Fig. 3a) LIDAR and ECE T_e profiles during RF heating.

Fig. 3b) LIDAR and ECE T_e profiles during Pellet Injection.